

Optimizing Surface Winds Using QuikSCAT Measurements in the Mediterranean Sea during 2000-2006

A. Birol Kara^{*}, Alan J. Wallcraft, Paul J. Martin,

*Oceanography Division, Naval Research Laboratory, Stennis Space Center, MS,
USA*

Randal L. Pauley

*Fleet Numerical Meteorology and Oceanography Center (FNMOC), Monterey, CA,
USA*

Abstract

Interannual variability of wind speed at 10 m above the sea surface is investigated over the Mediterranean Sea, with a particular focus near land-sea boundaries. For this purpose, monthly mean winds are formed at a resolution of 0.25° using twice-daily, rain-free, wind measurements calibrated to equivalent neutral winds from the QuikSCAT satellite during 2000-2006. A stability correction applied to these satellite-based winds reveals that the equivalent neutral winds are typically stronger by 0.2 m s^{-1} , and can even be stronger by $> 0.5 \text{ m s}^{-1}$ in some regions, including the Adriatic and Aegean Seas. Thus, the impact of air-sea stratification on the winds cannot be neglected, even on monthly time scales. Winds from a numerical weather prediction (NWP) model, the 0.5° -resolution Navy Operational Global Atmospheric Prediction System (NOGAPS), are found to have close agreement with the satellite-based winds. However, major differences arise near coastal boundaries where the winds from NOGAPS over the sea are contaminated by wind values over the land. Land-sea mask values from NOGAPS are introduced to examine the extent of the contamination, which can be severe (e.g., 2 m s^{-1} weaker) in comparison with QuikSCAT winds, especially near the northern boundaries. A creeping sea-fill methodology applied to the NOGAPS winds typically results in better agreement with the satellite winds. The accuracy of the NOGAPS winds is further improved by correcting them based on the satellite winds using a linear regression analysis. Finally, a 3.5-km-resolution HYbrid Coordinate Ocean Model (HYCOM) is forced with these original, sea-filled and regression-corrected NOGAPS winds. Sea-surface temperatures (SSTs) simulated by HYCOM demonstrate that the land-contaminated original winds from NOGAPS result in a relatively warm SST bias of $> 2^\circ\text{C}$ in comparison to a satellite-SST analysis near the coastal boundaries. Sea-filled and regression-corrected winds significantly improve the accuracy of the

SSTs from the model. The results presented in this paper clearly reveal that (1) stability dependence in the satellite winds cannot be ignored and (2) winds from a NWP product (NOGAPS here) over the sea may not be accurate near land-sea boundaries due to contamination by land values and can be improved either locally or via a regression against QuikSCAT winds.

Key words: Mediterranean Sea, Coastal Winds, QuikSCAT, Land Contamination, HYCOM

1 Introduction

Winds just above the sea surface play an important role in many features of the Mediterranean Sea. For example, as in many other parts of the global ocean, coastal upwelling near the land-sea boundaries of the Mediterranean Sea is mainly driven by winds (e.g., Olita et al., 2007). Ocean general circulation models (OGCMs) generally use wind forcing to simulate upper- and deep-ocean fields, including sea-surface temperature (SST) and surface circulation (e.g., Wu and Haines, 1996; Pinardi and Masetti, 2000).

For various offshore applications it is important to have accurate wind speed and direction at the sea surface (i.e., at 10-m height) over the Mediterranean Sea. High-temporal-resolution winds are typically available from numerical weather prediction (NWP) products. For example, the 1.125° European Centre for Medium-Range Weather Forecasts (ECMWF) provides archived wind output at 6-hourly intervals for 1979-2002 (Uppala et al., 2005), and the operational ECMWF fields are currently available at finer spatial resolution. Similarly, the Fleet Numerical Meteorology and Oceanography Center's global NWP model, the Navy Operational Global Atmospheric Prediction System (NOGAPS), as described in Rosmond et al. (2002), provides 0.5° resolution archived wind outputs at 3-hourly intervals since 2003, and the resolution 1.0° prior to 2003.

While temporal resolution of the winds from NWP products has great advantages, their coarse resolution has some shortcomings in typical applications in semi-enclosed seas, such as the Adriatic Sea. For example, Signell et al. (2005) discusses importance of using fine spatial resolution (e.g., 10-20 km) wind fields for oceanic applications. Kara et al. (2007) found that winds from the coarse-resolution NWP products can be quite inaccurate near land-sea boundaries when they are interpolated to much finer resolution. One obtains unrealistic winds from the interpolation because, near coastal regions, wind values over water are contaminated by values over land (and visa-versa) during interpolation to the finer grid, mainly because of the coarse atmospheric grid.

Wind measurements with finer spatial resolution than the global NWP products are available

* Corresponding author

Email addresses: birol.kara@nrlssc.navy.mil (A. Birol Kara),
alan.wallcraft@nrlssc.navy.mil (Alan J. Wallcraft), paul.martin@nrlssc.navy.mil (Paul J. Martin), randal.pauley@navy.mil (Randal L. Pauley).
URL: www7320.nrlssc.navy.mil (A. Birol Kara).

from the SeaWinds scatterometer sensor on the Quick Scatterometer (QuikSCAT) satellite over the global ocean since July 1999. The satellite-based QuikSCAT winds cover about 90% of the ice-free ocean each day, with an average of two observations per 25--km^2 grid cell each day (Wu et al., 2003). On the other hand, the winds from QuikSCAT have data voids, and they are calibrated to neutral atmospheric conditions and require air-sea stability correction to be consistent with those from the NWP products over the ocean. Although previous studies carefully analyzed QuikSCAT winds over the Mediterranean Sea, the impact of stability dependence on winds has been given little attention (e.g., Zecchetto and De Biasio 2007; Ruti et al. 2008).

The main purpose of this paper is four-fold: (1) to construct a rain-free QuikSCAT wind product at a resolution of 0.25° and quantify the impact of air-sea stratification on the winds during 2000-2006, (2) to provide a comprehensive analysis of wind speed variability based on the fine-resolution QuikSCAT and the relatively coarse-resolution NOGAPS data in the Mediterranean Sea, (3) to investigate the accuracy of winds near the land-sea boundaries by performing comparison between QuikSCAT and NOGAPS, and (4) to determine the accuracy of coastal and open-ocean SSTs simulated by an eddy-resolving OGCM that is forced with NOGAPS winds.

2 Stability Effects on Winds

SeaWinds scatterometer on the QuikSCAT satellite are used in our analyses from 2000 through 2006. For simplicity, these will be referred to as QSCAT winds throughout the text. All the surface winds presented in this paper are at the reference height of 10 m above the sea surface. For simplicity, we will hereafter drop the term 10 m and use only wind speed in place of wind speed at 10 m.

Scatterometers infer surface winds from the roughness of the ocean surface (Liu, 2002). Measurements of radar backscatter from a given location on the ocean surface are obtained from multiple azimuth angles as the satellite travels along its orbit. Scatterometers are calibrated to equivalent neutral wind speeds at 10 m above the ocean surface (Meissner et al., 2001) rather than the commonly-known wind speeds that include the effects of air-sea stability (i.e., stability-dependent winds).

Remote Sensing Systems (RSS) archives twice-daily fields of equivalent neutral winds at a grid resolution of 0.25° (<http://www.remss.com>). We use these archived wind data to convert equivalent neutral winds to stability-dependent winds. This is done to quantify the impact of atmospheric stability on the QSCAT wind values.

The conversion to stability-dependent winds was accomplished as follows: (1) We obtained near-surface atmospheric variables (ocean surface temperature, air temperature, and specific humidity at 10 m above the sea surface) from the 0.5° -resolution NOGAPS at 3-hourly intervals at each grid point over the Mediterranean Sea. (2) 12-hourly averages of all the near-surface atmospheric variables from NOGAPS were formed since QSCAT winds are available twice daily. (3) The 0.5° -resolution atmospheric variables were interpolated to the 0.25° QSCAT grid. (4) Based on a rain flag, equivalent neutral wind measurements that

have rain-contamination were eliminated since the existence of rain typically result in incorrect measurements from the scatterometer (e.g., Weissman et al., 2002), as will be further discussed below. (5) Finally, we used the near-surface atmospheric variables to convert the QSCAT rain-free equivalent neutral winds to stability-dependent winds at each grid point. The air-sea stability and resulting stability-dependent winds were computed with the Bourassa-Vincent-Wood (BVW) algorithm (Bourassa et al., 1999). The BVW model is a fully-coupled flux and ocean-state model. Coupling allows the ocean state to respond to atmospheric stability.

RSS directly provides monthly mean QSCAT wind speeds, but they are not constructed using twice-daily, rain-free wind measurements. All the winds, including the rain-contaminated ones, are used, and there is a cutoff of 20 observations per month (per 0.25° bin) for inclusion in the monthly mean field. However, many places have more than 20 rain-free observations. In our processing, as described in (1)-(5) above, only twice-daily, rain-free, wind measurements from QSCAT were used over the Mediterranean Sea. Monthly averages were formed on the 0.25° grid using a 25-point (1.25° square) observation-weighted average at each 0.25° cell using a cut-off of 100 rain-free observations per month. The 25-point average reduces the number of rain-contaminated cells but as a last step, all data voids, including land- and rain-contaminated cells, were filled using creeping sea-fill interpolation (Kara et al., 2007).

Following the procedure (1)-(5), spatial variability of the resulting stability-dependent QSCAT wind speeds converted from equivalent neutral winds is shown in January and July of 2006 (Figure 1a,b). These two months were chosen for illustrative purposes as representative of winter and summer, respectively. Winds in January are typically stronger than those in July over the Mediterranean Sea.

The impact of air-sea stability on the 10-m winds is examined in January and July of 2006, along with the same months of 2003, 2004, and 2005 (Figure 1). Differences between the stability-dependent and equivalent neutral winds are computed at 12-hour intervals, and monthly mean differences are then formed. Similar features are seen in all months, in that the stability-dependent winds are generally weaker than the equivalent neutral winds by about 0.2 m s^{-1} over most of the Mediterranean Sea. However, differences can be larger ($> 0.5 \text{ m s}^{-1}$) in some regions, such as the Adriatic and Aegean Seas. A difference of $\approx 0.2 \text{ m s}^{-1}$ is typical over the global ocean (Kara et al., 2008). In addition, Zecchetto and De Biasio (2007) report slight reduction in winds over the Mediterranean Sea after the stability correction was applied. We even found the stability-dependent winds are stronger than the equivalent neutral winds by $\approx 1 \text{ m s}^{-1}$ on 12-hour time scales (not shown). Errors associated with the methodology of stability-dependent correction are further discussed in Kara et al. (2008).

Hereinafter, stability-dependent QSCAT winds will be used throughout the paper. These are consistent with those provided by any NWP products, such as ECMWF and NOGAPS. Basin averages of monthly mean winds reveal a notable seasonal cycle in 2006 (Figure 2). They have values $> 7 \text{ m s}^{-1}$ during winter, weakening to about 5 m s^{-1} during spring and summer. There is some inter-annual variability in the winds as well (Figure 3). The common feature in all years is that the winds are relatively weak from June through September, and then get stronger in fall and winter.

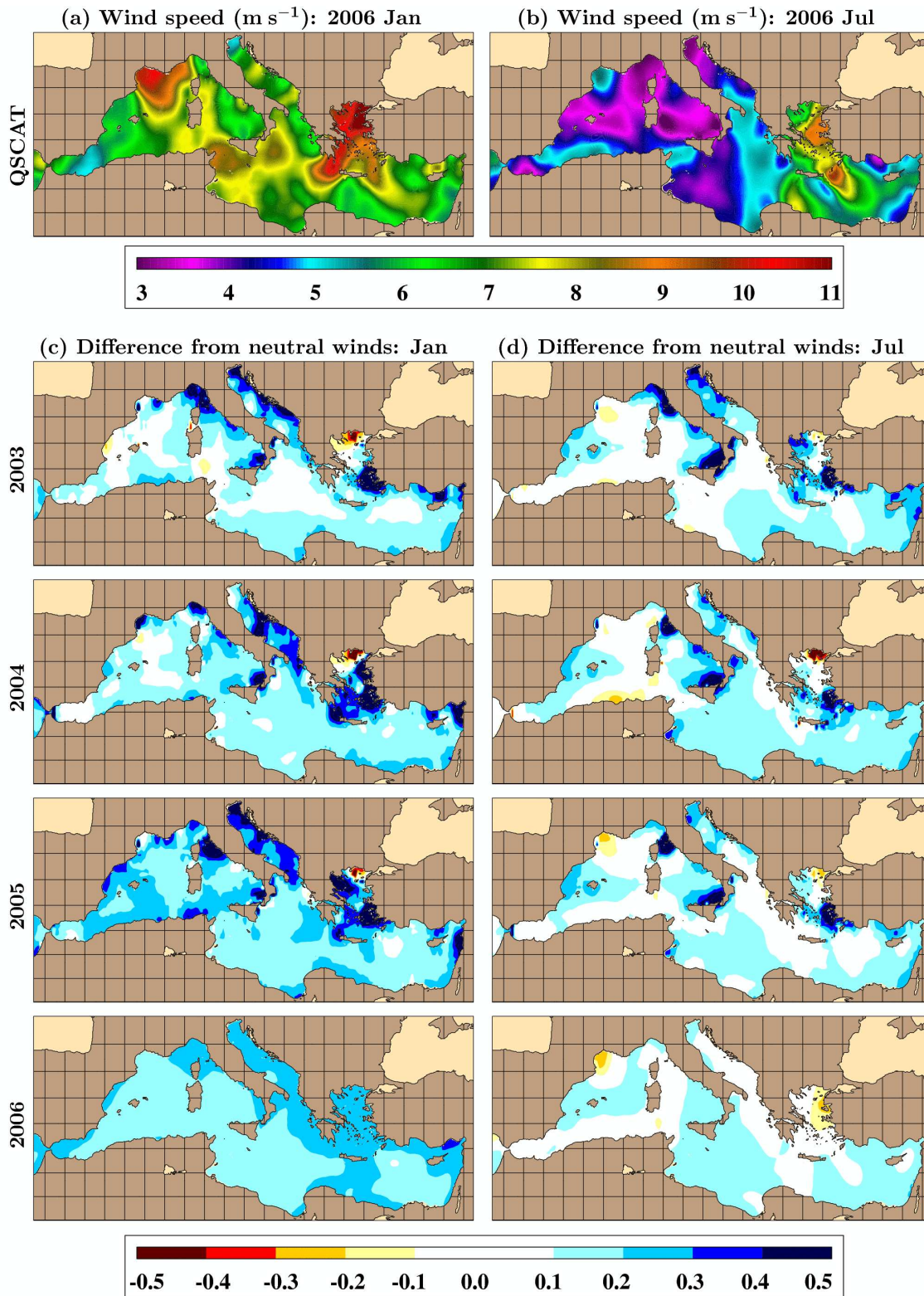


Fig. 1. Monthly mean winds from QSCAT in 2006: (a) January and (b) July. Monthly mean difference between equivalent neutral wind speed and stability-dependent wind speed in 2003, 2004, 2005 and 2006: (c) January and (d) July. The difference is calculated by subtracting stability-dependent winds from equivalent neutral wind speed.

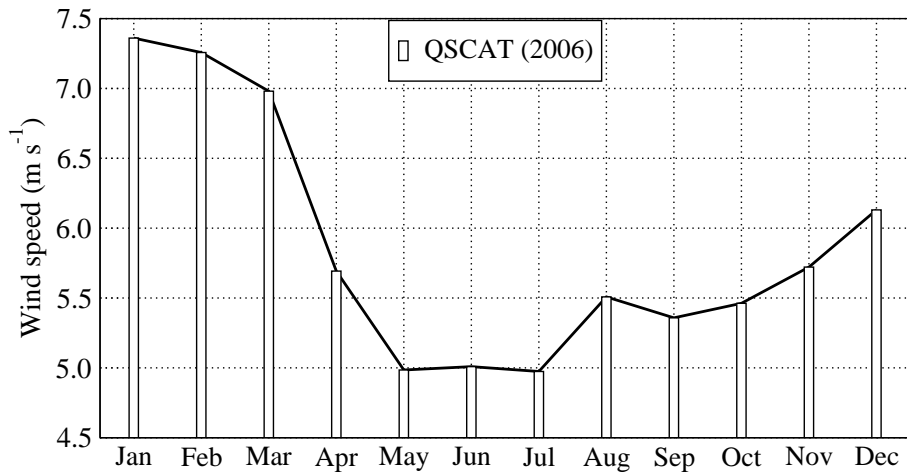


Fig. 2. Basin averages of stability-dependent QSCAT wind speeds by month over the Mediterranean Sea in 2006.

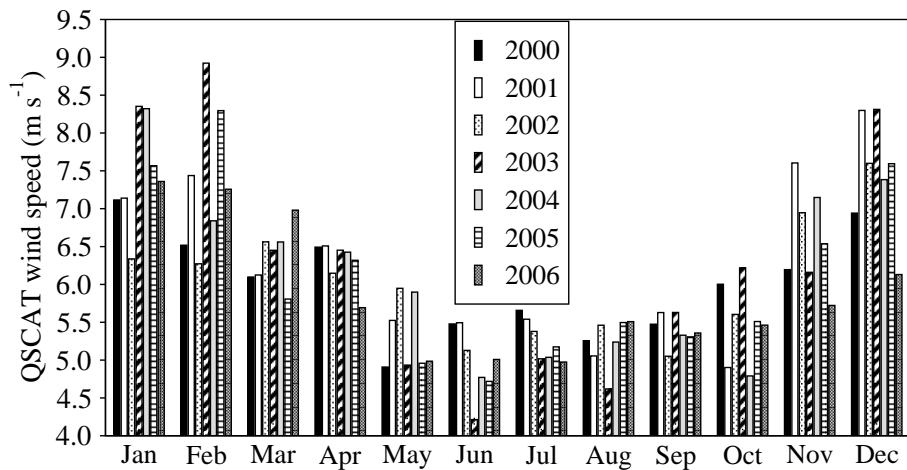


Fig. 3. Basin-averages of stability-dependent QSCAT winds speeds by month over the Mediterranean Sea from 2000 through 2006.

3 Land Contamination in Surface Winds

NOGAPS employs a planetary boundary layer formulation to calculate surface winds and wind stresses. wind speed observations over the ocean from the Special Sensor Microwave/Imager (SSM/I) instrument and the ERS-2 scatterometer provide a particularly important source of data for assimilation. QSCAT winds have also been assimilated into NOGAPS since 2004.

Since the beginning of 2003, NOGAPS has provided archived fields at high (3 hour) temporal resolution on its “computational” 0.5° grid. This is an improvement over the common practise among NWP products of distributing fields on a standard coarser resolution grids. Non-nature grids can pose a problem when using the fields for coastal applications since (i) values near the land-sea boundary can be influenced by both land and sea effects and, as a result, the gradient from land to sea can be very large and (ii) interpolation of the fields from one grid to another tends to smear (spread out) the transition from land values to sea values. Hence, if one is concerned with values over the sea (land), these will be “contaminated” by values from land (sea) points on the original grid near land-sea boundaries.

3.1 Land-Sea Mask in the Mediterranean Sea

The amount of intrinsic contamination in the winds or other near-surface atmospheric variables from a NWP product like NOGAPS is mainly related to the land-sea mask. To demonstrate the amount of land contamination in the winds or in the other near-surface variables from NOGAPS, we interpolated the land-sea mask values from the 0.5° NOGAPS grid to a much finer grid of $1/25^\circ \cos(\text{lat}) \times 1/25^\circ$ (i.e., a resolution of about 3.5 km). This grid will later be used for OGCM simulations of SST.

The NOGAPS land-sea mask values interpolated just to the sea points of the finer grid are shown for the Mediterranean Sea along with three sub-regions (Figure 4a). A land-sea mask value of 0.7, for example, implies that the fields interpolated to this grid point get 70% of their value from land points and 30% of their value from ocean points on the original grid, i.e., the values are about 70% contaminated by land values. There are some locations in the western Aegean Sea where the land contamination can be as high as 100%.

Unlike NOGAPS, the land-sea mask for QSCAT has a different meaning since all the QSCAT measurements are over the water (i.e., there is no land contamination for QSCAT winds). We define the land-sea mask for QSCAT based on the availability of twice-daily wind measurements from the satellite for a given month. On a month-by-month basis, the mask could vary depending on the orbital pattern. The land-sea mask is 1.0 for data-void areas and 0.0 for regions with valid QSCAT winds. For example, there are not many available wind measurements from QSCAT near the coastal regions of the Mediterranean Sea in January 2005 (Figure 4b).

In the case of the Aegean Sea, there are many locations where no wind measurements were available. While the QSCAT land-sea mask varies by month, this is typical for this particular region in all months from 2003 through 2006 (not shown). The main reason for having limited or no measurements in such regions is the failure of the satellite to determine the winds accurately. This is caused by the fact that the QSCAT footprint is an ellipse approximately 25-km in the cross-track and 37-km in the along-track direction. In regions where there are irregular coastlines, such as the Aegean Sea, the footprint includes land areas, and thereby the backscatter from the land areas gives inaccurate winds.

3.2 Mean Bias Between NOGAPS and QSCAT Winds

monthly mean NOGAPS winds were constructed based on 3-hourly archived outputs under three categories (Table 1). Each of these products will later be used for forcing an OGCM in Section 4. All of these original and post-processed winds are interpolated to the $1/25^\circ \cos(\text{lat}) \times 1/25^\circ$ grid from the original, 0.5° NOGAPS grid.

In the table, NOGAPS-std represents the standard (i.e., original) winds. The winds for NOGAPS-sea are obtained based on the creeping sea-fill technique whose details are given in Kara et al. (2007). The purpose of this technique is to reduce land contamination near the land-sea boundaries. The creeping sea-fill technique first uses only over-sea values of wind speed, i.e., those just outside the land-sea mask where there is no land contamination (see

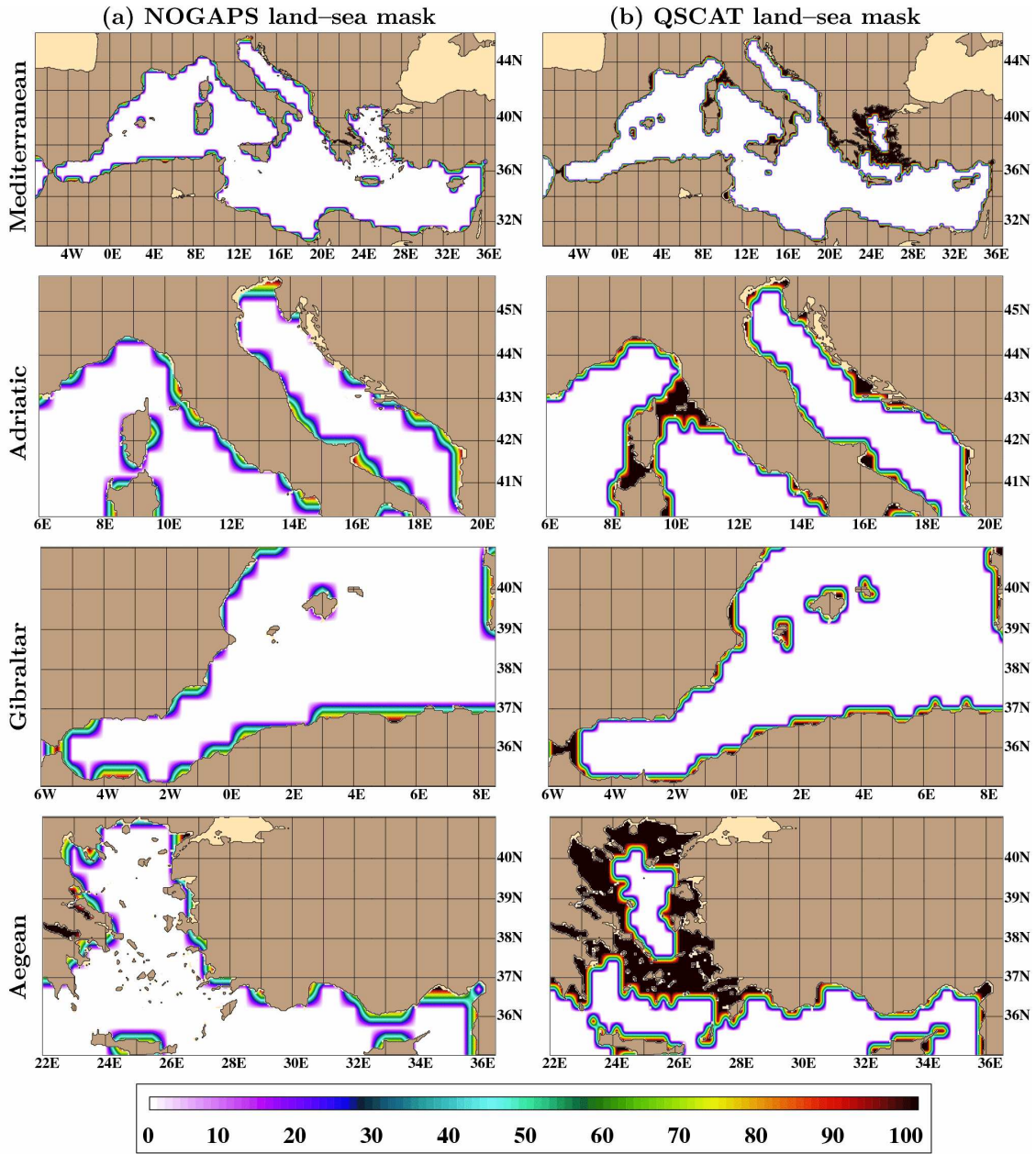


Fig. 4. Land-sea mask values from (a) NOGAPS and (b) QSCAT. They are interpolated to $1/25^\circ \cos(\text{lat}) \times 1/25^\circ$ grid for illustration purposes. Land-sea mask values are shown for the whole domain and three sub-regions. The color bar demonstrates the percentage amount of land contamination. Simply, similar to other NWP products, the ocean and land areas in NOGAPS are defined by a land-sea mask with 0 for sea and 1 for land. A grid point (cell) is defined as a land point if more than 50% of the actual surface of the grid cell is land.

the white colors in Figure 4a). The methodology is then to replace the value associated with each land-masked point using the mean of the values at the adjoining sea points.

To form the winds for NOGAPS-reg based on NOGAPS-sea, as given in Table 1, we perform a linear regression analysis between the monthly mean NOGAPS-sea and QSCAT winds at each grid point (i.e., $\text{NOGAPS} = a\text{QSCAT} + b$, where a is the slope, and b is the intercept in m s^{-1}). This is based on the fact that these winds are highly correlated with correlation coefficients of > 0.9 based on a time series of 48 monthly mean winds almost everywhere over the Mediterranean Sea from 2003 through 2006 (Figure 5a). The slope and intercept

Table 1

Wind speed products from NOGAPS and their abbreviations used throughout the text.

| Wind product | Description |
|--------------|---|
| NOGAPS-std | Original winds directly obtained from NOGAPS |
| NOGAPS-sea | Creeping sea-fill applied on NOGAPS-std wind |
| NOGAPS-reg | Regression analysis applied on NOGAPS-sea winds |

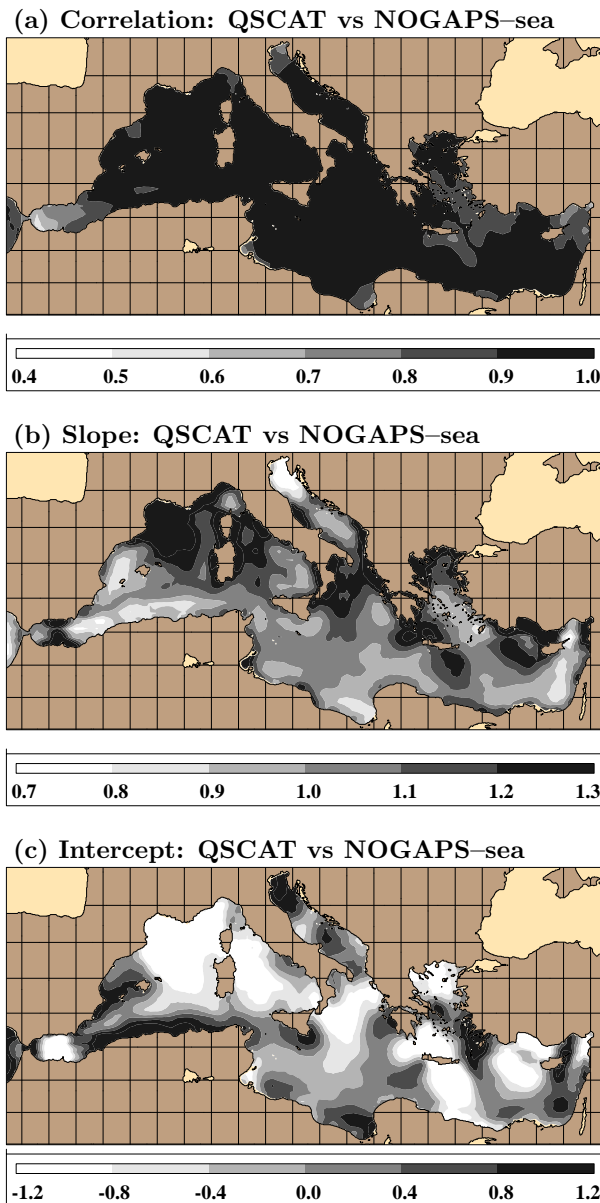


Fig. 5. (a) Linear correlation coefficients between NOGAPS-sea and QSCAT winds calculated over the 4-year time period during 2003-2006. (b) Slope values of the least squares lines. (c) Intercept values (in m s^{-1}) of the least squares lines.

values for the least squares lines are then computed at each grid point (Figure 5b,c). Hence, the NOGAPS-sea winds are re-calibrated as NOGAPS-reg winds.

The purpose of this regression correction is to reduce possible errors in the NOGAPS winds under the assumption that the QSCAT winds represent the truth. This is necessitated by the fact that one cannot use the twice-daily QSCAT winds directly in an OGCM simulation

since there can be data voids, depending on the coverage of the satellite passes. However, a correction based on the QSCAT monthly means can improve the accuracy of the 3-hourly NOGAPS winds (Section 4), which can then be used for forcing an OGCM.

A comparison of all the wind products, including those for NOGAPS and QSCAT, is performed in January for three different years: 2003, 2004, and 2005 (Figure 6). As mentioned in Section 2, the monthly QSCAT winds were formed from twice-daily wind measurements. A creeping sea-fill was also applied to them based on the QSCAT land-sea mask (e.g., see Figure 4b). The winds for NOGAPS-std were obtained from the 3-hourly archived outputs. The NOGAPS-sea and NOGAPS-reg fields were constructed based on the NOGAPS-std fields at each 3-hourly time interval and then averaged over a month.

The most obvious feature evident from Figure 6a is that the inter-annual variability in QSCAT is successfully replicated by all three NOGAPS products. For example, the winds from QSCAT are relatively weaker (stronger) in the easternmost part of the Mediterranean Sea in 2003 (2005). NOGAPS-reg has the advantage of reproducing the QSCAT winds. This can be seen in the northwestern part of the region where the QSCAT winds are generally stronger by $> 2 \text{ m s}^{-1}$. Unlike NOGAPS-std and NOGAPS-sea, such strong winds are evident in NOGAPS-reg.

Major differences between the QSCAT and NOGAPS winds arise near the coastal regions (Figure 6b). The NOGAPS-std winds are too weak, especially near the northern boundaries. The NOGAPS-sea winds, which were formed based on the creeping sea-fill methodology, are effective in reducing the biases near the land-sea boundaries. Here we note that the Aegean Sea is a region where even the QSCAT wind measurements are not very reliable near coastal regions as discussed earlier (see Figure 4).

To better illustrate land contamination in the winds near coastal boundaries, monthly mean differences for 2005 are computed based on the extent of the land-sea mask from NOGAPS. The words “all ocean“ in Figure 7 indicate that the areal averages of the wind speed differences (NOGAPS-QSCAT) for each wind type (i.e., std, sea, and reg) were computed within the region where there is no land contamination, i.e., all the land-sea mask values have 0’s (see Figure 4a). Similarly, the word “mask“ in Figure 7 indicates that the wind bias was obtained in the regions within the land-sea mask having values of > 0 to 1.0. The land-sea mask value of $> 20\%$, for example, represents differences where the land contamination in the winds is between 20% and 100%, i.e., the land-sea mask values are between 0.2 and 1.0.

As evident from Figure 7, the winds from NOGAPS-std and NOGAPS-sea are identical for the all-ocean points since the creeping sea-fill has no effect at these points. When considering areal averages of wind speed differences for all the land-contaminated regions, within the mask, the sea-filled winds from NOGAPS-sea have smaller biases compared to those from NOGAPS-std. In the presence of 80% or more land contamination, winds from NOGAPS-sea can even be as weak as $4\text{-}5 \text{ m s}^{-1}$ in comparison with those from QSCAT. While NOGAPS-sea winds reduce this bias, the major improvement is obtained from NOGAPS-reg.

The existence of too weak winds from NOGAPS-std based on various land-sea mask class intervals, discussed in the preceding paragraph for only 2005, is sought in other years. A scatter diagram of areally-averaged monthly mean wind speed differences is produced over the 48-month time period during 2003-2006 when the land contamination is between 20%

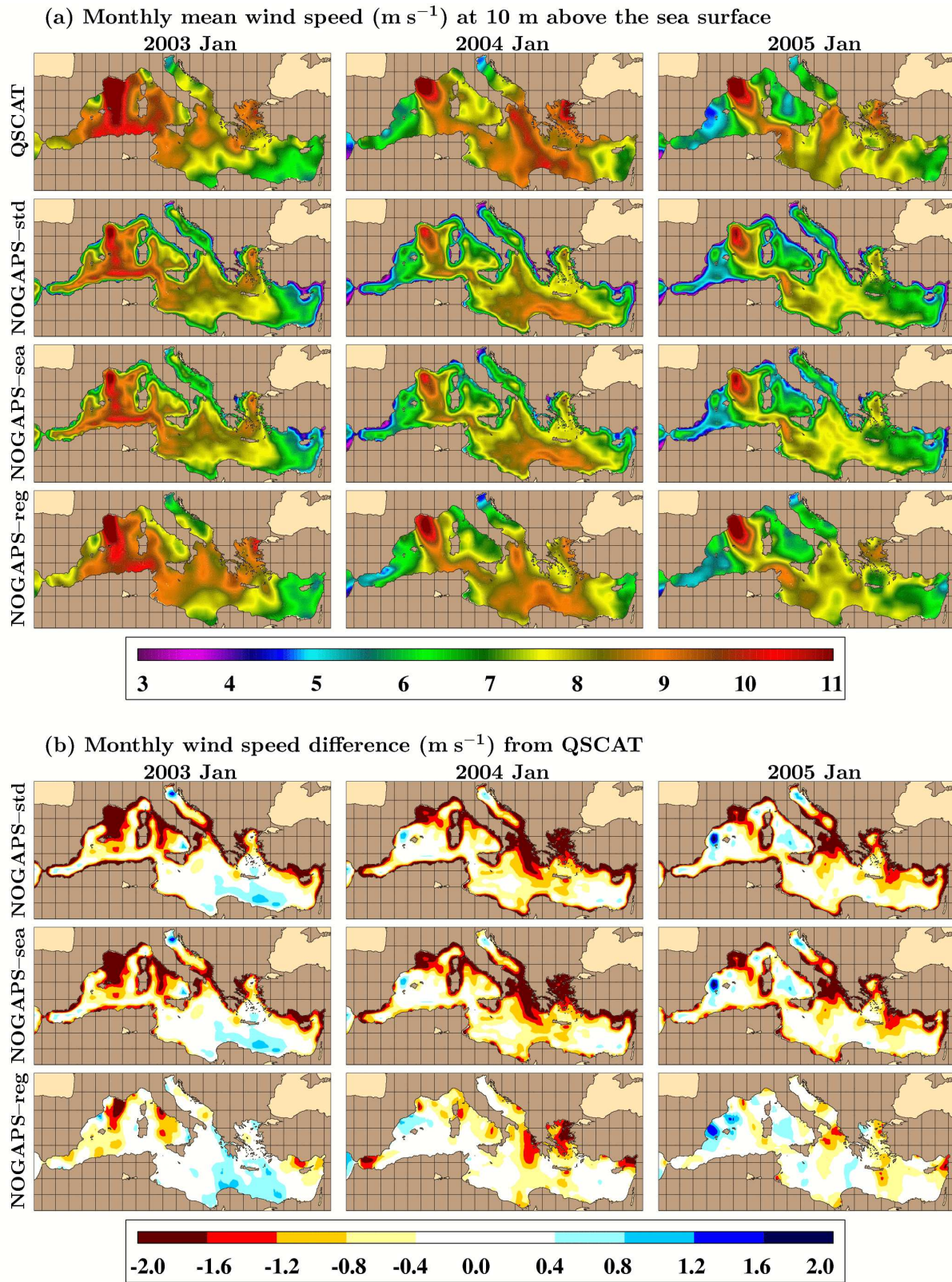


Fig. 6. (a) Monthly mean wind speeds from QSCAT and three NOGAPS products in January of 2003, 2004 and 2005. (b) Wind speed difference (i.e., NOGAPS-QSCAT) for the fields shown in (a). Differences are computed for each NOGAPS product.

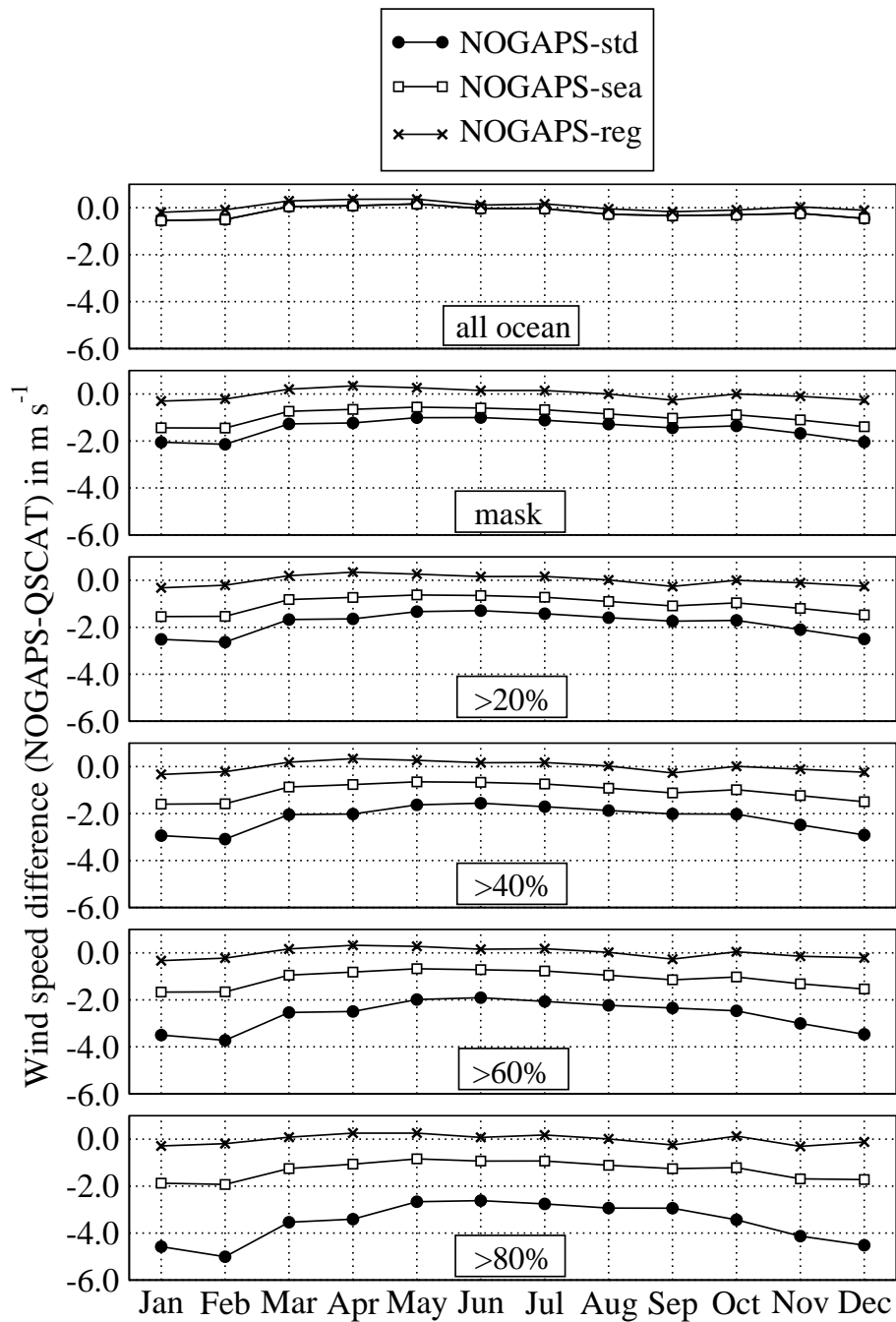


Fig. 7. Monthly mean wind speed differences (NOGAPS-QSCAT) calculated using original, sea-filled and regression-corrected NOGAPS products in 2005. The results are shown for all ocean points (i.e., no land contamination), all land-contaminated points (i.e., mask) and various categories of land-sea mask values as explained in the text.

and 100% (Figure 8). The mean biases with respect to the QSCAT winds are 1.8, 1.0, and 0.1 m s^{-1} for NOGAPS-std, NOGAPS-sea, and NOGAPS-reg, respectively. Such biases for the original NOGAPS winds are even larger very near the coast, e.g., when the land contamination is between 80% and 100% (Figure 9). In particular, the mean wind speed differences are 4.2, 2.1, and 0.5 m s^{-1} . The sea-filled winds did not perform as well as the regression-corrected winds because the accuracy of the former methodology depends on the accuracy of the NOGAPS winds in the interior of the ocean used for interpolating the winds.

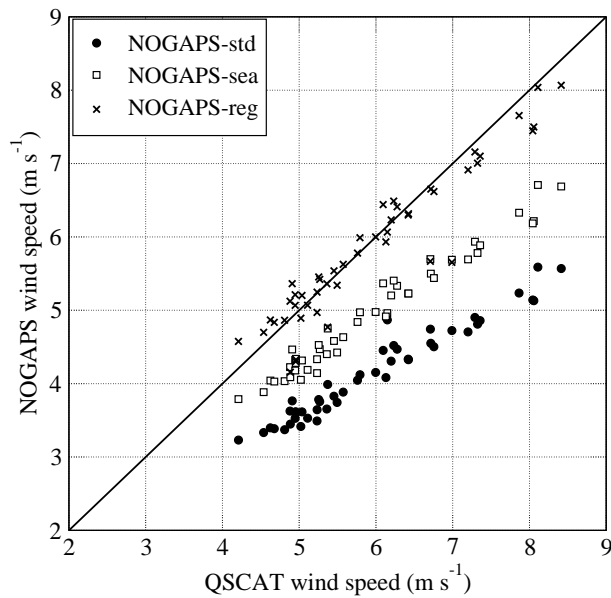


Fig. 8. Scatter plot of monthly mean winds between QSCAT and each one of NOGAPS products during 2003-2006 when the areally-averaged winds are computed in the regions where land contamination is $> 20\%$ over the Mediterranean Sea.

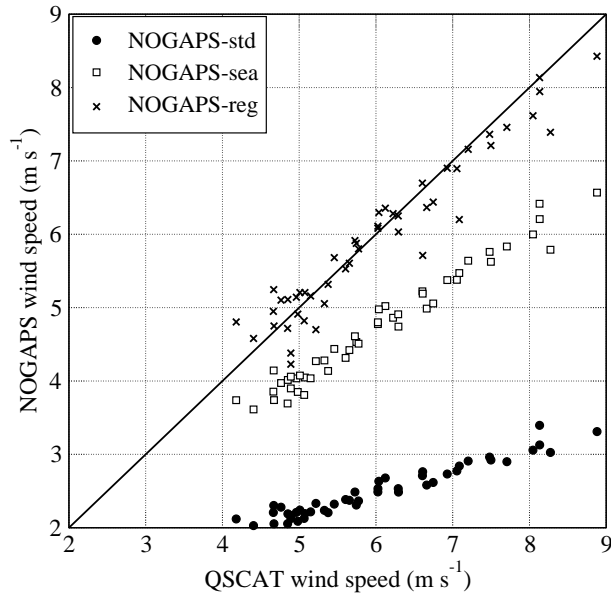


Fig. 9. The same as Figure 8 but for land contamination of $> 80\%$, i.e., very near the coast, over the Mediterranean Sea.

3.3 Land Contamination in the Adriatic Sea

Since the differences in the winds between QSCAT and each of the NOGAPS products near land-sea boundaries are not clearly seen in Figure 6, we further analyze the winds in a smaller region that includes the Adriatic Sea. Previously, Cavaleri and Bertotti (1997) found that orography has a strong influence on the wind variability in the Adriatic Sea, making this region a good candidate for such an investigation. The QSCAT winds are almost uniform with a value of about 4 m s^{-1} in the northern Adriatic Sea, i.e., the winds near the coastal boundaries do not differ from those in the interior in July 2005 (Figure 10a). There are only

a few locations where the QSCAT wind measurements, used for forming monthly means, were not available as evident from the land-sea mask value of 100% (Figure 10b).

Unlike QSCAT, winds from NOGAPS-std are too weak (about 2 m s^{-1}) near all the land-sea boundaries in July 2005 (Figure 10c). The land contamination for NOGAPS winds in this region typically extends farther into the interior in comparison to QSCAT as already shown in Figure 4a. The land-sea mask for NOGAPS is also similar in July 2005 (not shown) since the QSCAT footprint typically sees the same regions during each pass. The creeping sea-fill is certainly effective in improving the accuracy of the winds in this particular region since the winds from NOGAPS-sea become stronger by about 1 m s^{-1} than those from NOGAPS-std. However, the sea-filled winds are still weak in comparison to the QSCAT winds because of the fact that the NOGAPS winds just outside the land-sea mask ($\approx 3 \text{ m s}^{-1}$) are not as strong as the QSCAT winds.

The application of linear-regression analysis to the NOGAPS-std winds clearly provides the best agreement with respect to QSCAT (Figure 10d). For example, even the sea-filled winds have some biases in the southern Adriatic Sea, however, they are within $\pm 0.4 \text{ m s}^{-1}$ of the winds from NOGAPS-reg. Some of the NOGAPS low speed bias in the Adriatic (and elsewhere) may be attributable to insufficient resolution for modeling orographically influenced mesoscale circulations. Although NOGAPS-reg properly remediates such deficiencies, another approach that might be considered in future is the use of a mesoscale NWP model, such as the U.S. Navy Coupled Atmospheric Mesoscale Prediction System (COAMPS).

3.4 Basin-Wide Wind Speed Comparisons

In this section, we evaluate basin-wide averages of the winds from QSCAT and all three NOGAPS products. Monthly means were computed for each year from 2003 through 2006. As an example, Figure 11 shows time series of basin-averaged, monthly mean winds from all the products in 2005. The NOGAPS-std winds are weaker than those of the other products. Not surprisingly, the land-contaminated coastal winds contribute much of the difference as discussed in the preceding section. The basin-averaged, annual-mean wind speed is 6.1 m s^{-1} for both QSCAT and NOGAPS-reg, illustrating the success of the regression-corrected NOGAPS product.

Finally, we combine the basin-averaged, monthly mean winds from each product for all the years during 2003-2006 and produce a scatter plot between QSCAT and each of the NOGAPS products (Figure 12). There are a total of 48 monthly mean wind values during the 4-year time period. The winds from NOGAPS-std are clearly much weaker than those from QSCAT by 0.6 m s^{-1} . There is a moderate improvement in the NOGAPS-std winds from the creeping sea-fill, evident in the smaller scatter of the NOGAPS-sea winds. The most significant improvement is evident from the NOGAPS-reg winds, resulting in values almost identical to the QSCAT winds. In fact, the mean bias between the basin-averaged QSCAT and NOGAPS-reg winds is zero during 2003-2006.

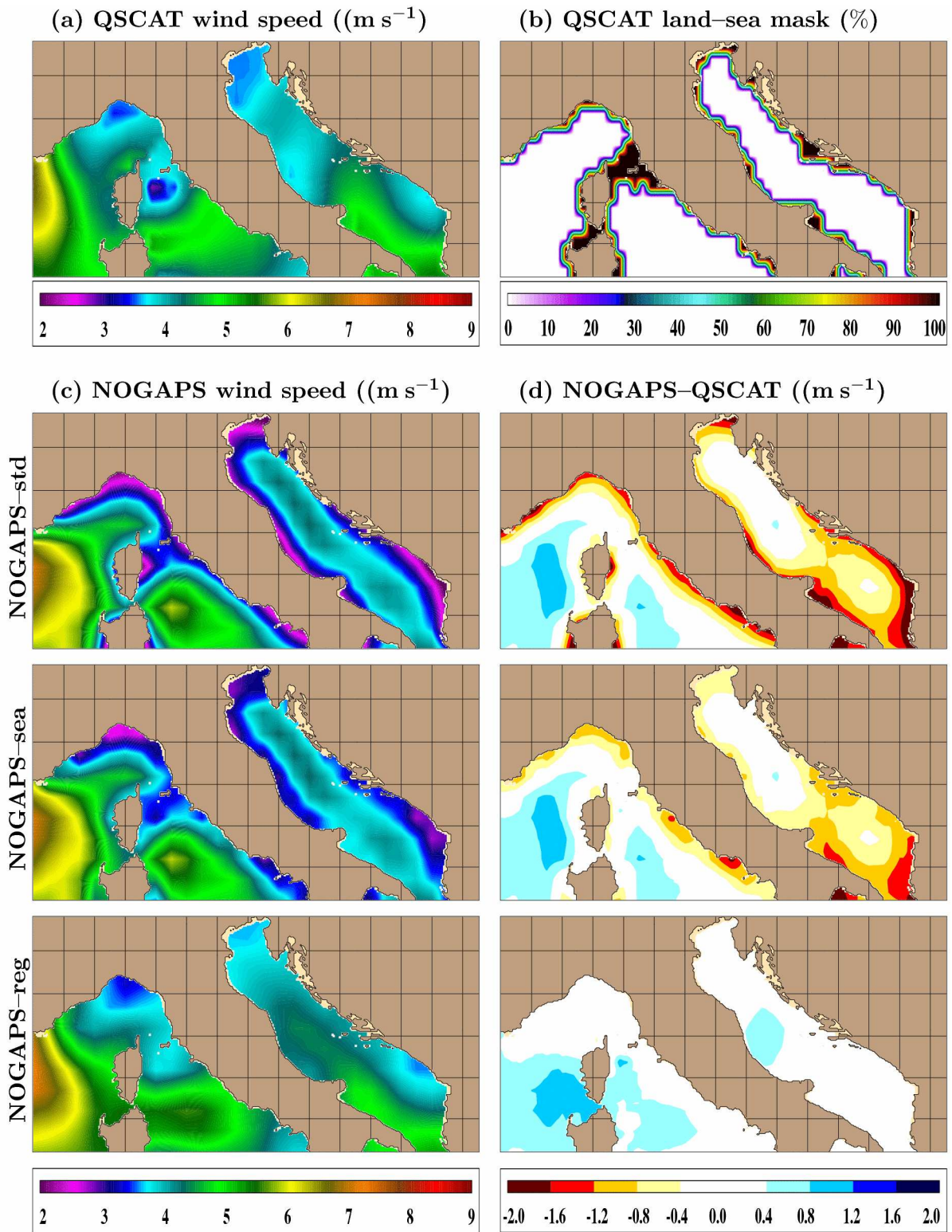


Fig. 10. (a) Monthly mean winds from QSCAT in the region involving the Adriatic Sea in July of 2005. (b) Land-sea mask for QSCAT winds. A value of 100% indicates that there are no wind measurements from the SeaWinds scatterometer on the QuikSCAT satellite. (c) Monthly winds from NOGAPS in July of 2005. (d) Difference for NOGAPS winds, i.e., NOGAPS winds subtracted from QSCAT in July of 2005.

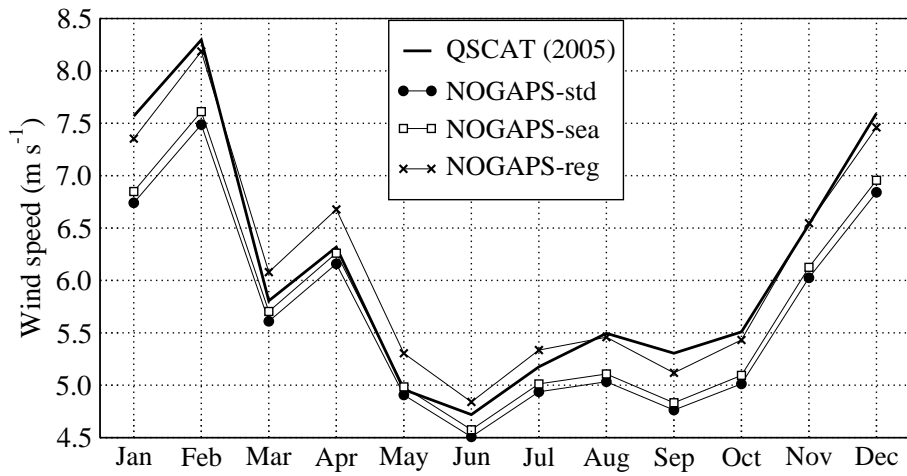


Fig. 11. Time series of basin-averaged monthly mean wind speed from QSCAT and three NOGAPS products in 2005. Basin-averaged annual mean wind speeds are 6.1, 5.7, 5.8 and 6.1 m s^{-1} for QSCAT, NOGAPS-std, NOGAPS-sea and NOGAPS-reg, respectively.

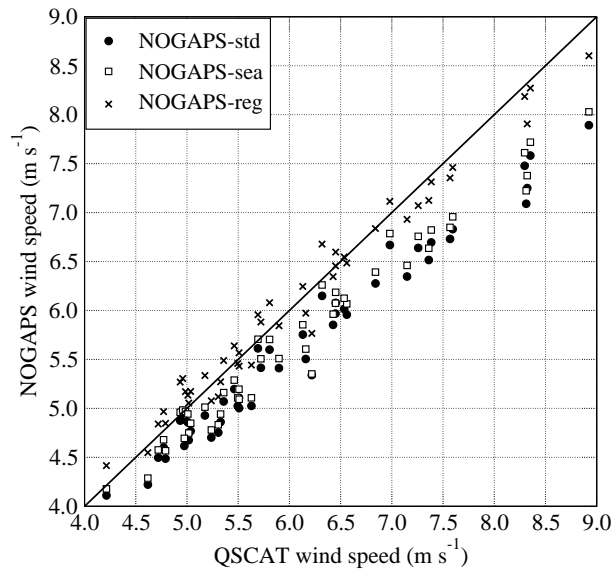


Fig. 12. Scatter plot of basin-averaged monthly mean QSCAT versus each type of NOGAPS winds. Monthly winds are shown for all years from 2003 through 2006.

4 The Impact of Winds in Simulating Mediterranean SST

The winds from NOGAPS-std, NOGAPS-sea, and NOGAPS-reg introduced in section 3 are used to force an OGCM, and the impact of each wind product on the OGCM’s simulated SST near the coastal boundaries and in the open-ocean areas of the Mediterranean Sea is examined.

4.1 Ocean Model

The OGCM we use is the HYbrid Coordinate Ocean Model (HYCOM). It is a community ocean model (<http://oceanmodeling.rsmas.miami.edu/hycom/>). HYCOM behaves like a conventional σ (terrain-following) model in very shallow oceanic regions, like a z -level

(fixed-depth) coordinate model in the mixed layer or other unstratified regions, and like an isopycnic-coordinate model in stratified regions. For the simulations conducted here, vertical mixing was computed using the K-Profile Parameterization (KPP) of Large et al. (1997).

The Mediterranean Sea HYCOM was configured with a resolution of $1/25^\circ \cos(\text{lat}) \times 1/25^\circ$ (latitude \times longitude) on a Mercator grid. The Mercator projection has square grid cells of about $0.04 \times \cos(\text{lat}) \times 111.2$ km in each direction. The mean horizontal grid resolution is about 3.5 km. There are 20 hybrid layers in the vertical (the setup of the vertical grid is further explained in Appendix I.1).

Temperature and salinity from the $1/4^\circ$ Generalized Digital Environmental Model (GDEM) monthly climatology developed at the Naval Oceanographic Office (NAVOCEANO) was used for relaxation in the small Atlantic portion of the domain to obtain the correct flow through the Strait of Gibraltar. The monthly GDEM climatology was also used for relaxation of the sea-surface salinity (SSS) to keep the surface salinity balance on track.

The net heat flux absorbed from the sea surface down to depth z is parameterized following Kara et al. (2005a), and the rate of heating/cooling of each model layer can be computed. The sensible and latent heat fluxes are calculated using HYCOM's upper-layer temperature at each model time step using bulk formulae that include the effects of dynamic stability (Kara et al., 2005b). The reader is also referred to Appendix I.2.

HYCOM uses 3-hourly atmospheric forcing data from the 0.5° NOGAPS (Rosmond et al., 2002). The wind forcing includes the zonal and meridional components of the wind stress at the air-sea interface and the scalar wind speed at 10 m above the sea surface. Wind stresses are computed based on 10 m winds from NOGAPS based on the bulk formulation. The thermal forcing involves the air temperature and specific humidity at 10 m above the sea surface, along with net shortwave and longwave radiation fields absorbed at the sea surface.

4.2 HYCOM Simulations

The model was first run using wind and thermal forcing from NOGAPS from 2001 until 2003. This time period was used as a spin up. The model simulation was then extended using 3-hourly atmospheric forcing. There are three HYCOM simulations performed from 2003 through 2006. These are expt 1, expt 2, and expt 3, which were forced with winds from NOGAPS-std, NOGAPS-std, and NOGAPS-reg, respectively. Since we would like to investigate the impact of the winds on the model simulations, the thermal forcing variables (other than the wind speed) were the same for all the simulations. The creeping sea-fill methodology is applied to all the thermal forcing variables to reduce the land contamination before using them for the model simulations.

4.3 Sensitivity of SST to Land Contaminated Winds

SSTs obtained from the HYCOM simulations are compared to those from an analysis of satellite SSTs. The accuracy of the SST determined from these comparisons gives us a basis

for judging which of the wind products results in a better simulation. Thus, one can decide which wind product is optimal near the land-sea boundaries and in the interior.

The SST is used for the validations since it is one of the best-observed oceanic fields, i.e., one can obtain SSTs at high temporal (e.g., daily) and fine spatial (e.g., 0.5°) resolution. In this study, daily SSTs were obtained from the $1/8^\circ$ -resolution Modular Ocean Data Analysis (MODAS) re-analysis over the global ocean (Kara and Barron, 2007). The MODAS SSTs were interpolated to the Mediterranean Sea HYCOM domain and used to form monthly means during 2003-2006. Similarly, monthly mean SSTs from the HYCOM simulations were constructed from daily model outputs during the same time period.

Monthly and annual mean SST biases and RMS SST errors are computed for 2003-2006. Let X_i ($i = 1, 2, \dots, n$) be the set of monthly mean MODAS SST values from January to December in a given year, and let Y_i ($i = 1, 2, \dots, n$) be the set of corresponding HYCOM predicted SSTs at a given model grid point. The mean bias is $\bar{Y} - \bar{X}$, and the RMS SST error is $\left[\frac{1}{n} \sum_{i=1}^n (Y_i - X_i)^2\right]^{1/2}$. These metrics are computed at each grid point over the annual cycle for a given year, thus, for example, n is 12 in 2003. When evaluating results during 2003-2006, n is set to 48.

In Figure 13, the spatial variation of the mean bias and RMS error are shown for expts 1, 2, and 3 forced with winds from NOGAPS-std, NOGAPS-sea, and NOGAPS-reg, respectively. We first examine errors in an individual year, 2005, so statistical values were calculated based on 12 monthly mean SST time series from HYCOM and MODAS (Figure 13a,b). In expt 1, there are clearly relatively large model SST biases of $> 1^\circ\text{C}$ and RMS errors of $> 2^\circ\text{C}$ near most of the coastal boundaries in 2005. Note that a warm SST bias from HYCOM also exists in the interior.

In comparison to NOGAPS-std winds, the sea-filled winds used for forcing HYCOM gave slightly better SSTs near the coastal boundaries. As expected, the mean SST bias and RMS error between expt 1 and expt 2 remained almost the same in the interior because NOGAPS-sea winds are identical to NOGAPS-std winds everywhere except near the land-sea boundaries. We should indicate that some of the model SST errors are not directly related to the wind forcing, and can be due to dynamical processes related to the model parameterizations. Here, we limit ourselves to examining the impact of wind forcing errors on the model simulations. The model which is forced with winds from NOGAPS-reg in expt 3 clearly gives the smallest mean bias and RMS SST error. SST errors from the model are reduced not only near the land-sea boundaries but also farther from the coastal regions, i.e., in the interior.

The evaluation of the HYCOM simulations for 2005 was repeated for the 4-year time period 2003-2006 (Figure 13c,d). This was done to examine the SST error characteristics over a longer time period. Based on 48 monthly mean, SST time series comparisons between HYCOM and MODAS, the results reveal that the mean bias and RMS errors are almost the same as those for 2005. Similar to the fields shown in Figure 13a,b, the relatively large SST mean biases and RMS errors in expt 1 forced with winds from NOGAPS-std are again seen near most of coastal boundaries of the southern Mediterranean Sea. SST errors also exist in the interior. Most of these errors near and far away from the coast were greatly reduced in expt 3 in which HYCOM was forced with winds from NOGAPS-std.

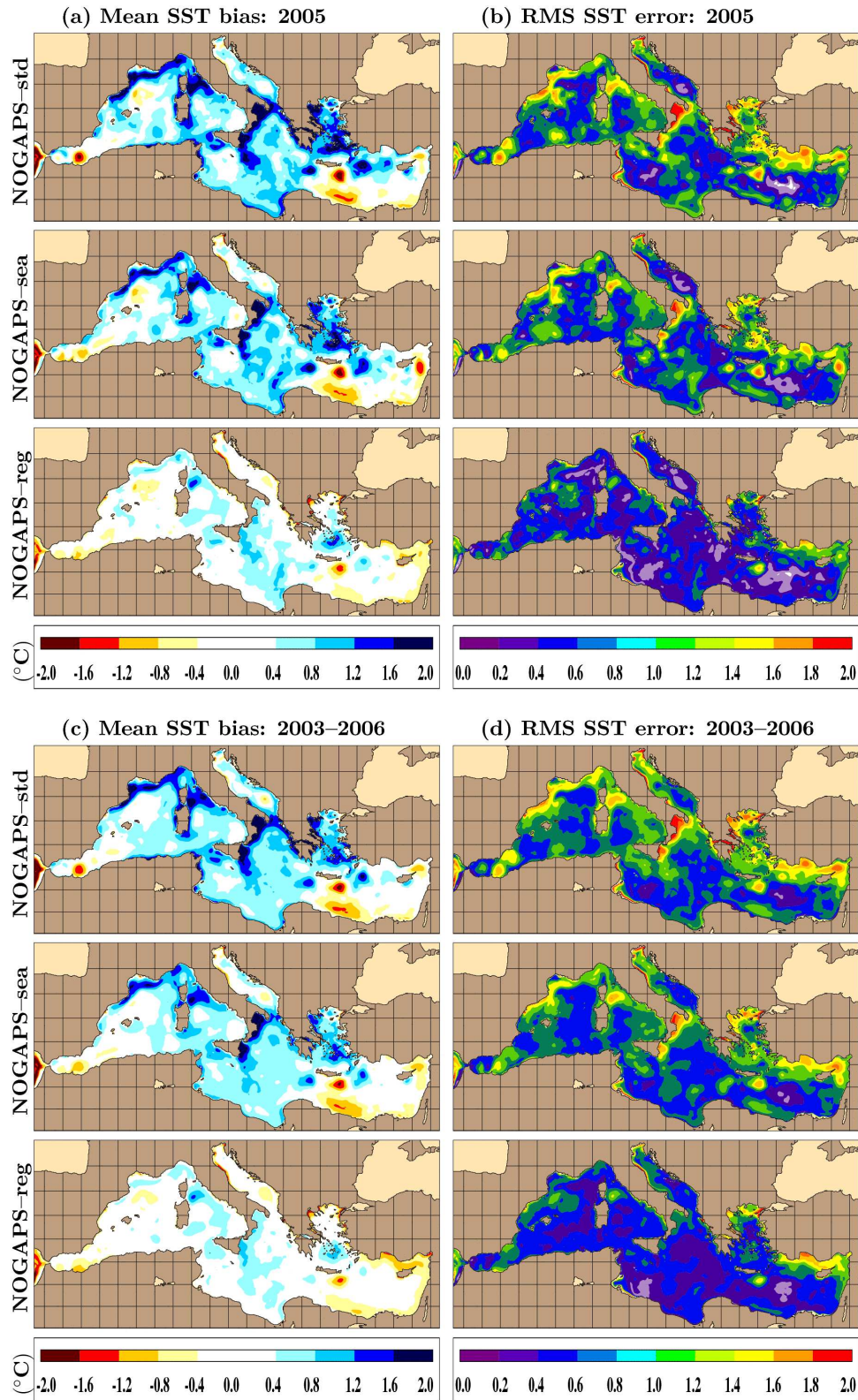


Fig. 13. Statistical evaluation of monthly mean SST between HYCOM and MODAS when HYCOM was forced using winds from original, sea-filled and corrected NOGAPS products: (a) SST bias (HYCOM-MODAS) during 2005, (b) RMS SST error between HYCOM and MODAS during 2005, (c) the same as (a) but during 2003-2006, and (d) the same as (b) but during 2003-2006.

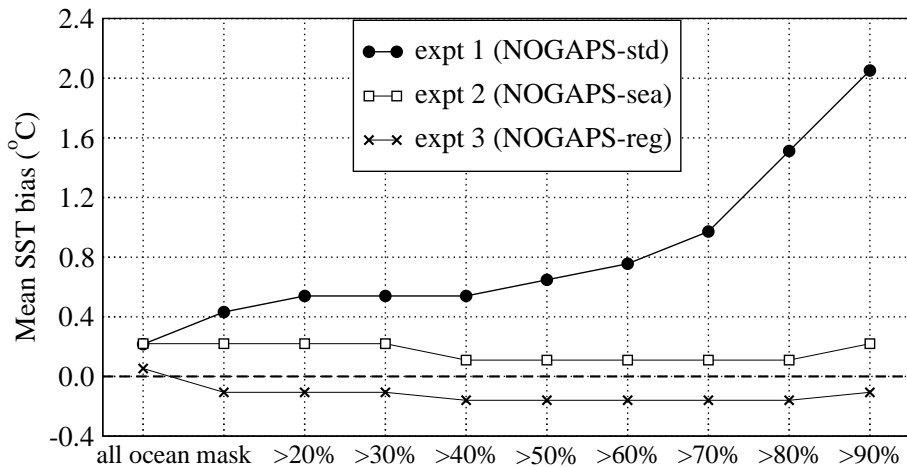


Fig. 14. Areal averages of mean SST bias (HYCOM-MODAS) computed over the 4-year time period (48 months) in the Mediterranean Sea 2003 through 2006. Areal averages are calculated based on the extent of the land-sea mask values. See text for details.

To gain more insight into the impact of the winds in simulating SST near the land-sea boundaries and away from the coast, we computed mean SST biases based on the extent of the land-sea mask from NOGAPS. The mask values are already shown in Figure 4a. In particular, areal averages of the mean SST biases between HYCOM and MODAS were calculated for the locations outside the land-sea mask, within the land-sea mask, and for various categories of land-sea mask values during 2003-2006 (Figure 14).

We use “all ocean“ on the x-axis of Figure 14 to indicate that the areal averages of the SST bias (HYCOM-MODAS) were computed for the locations where there is no land contamination, i.e., where all the land-sea mask values have 0’s. Similarly, the word, “mask“, on the x-axis means the mean bias was computed using time series of SST just in the regions where the land-sea mask has values > 0 . The value of $> 20\%$, for example, represents SST biases where the land contamination of the winds is between 20% and 100%, i.e., the land-sea mask values are between 0.2 and 1.0.

Clearly, the SST biases from HYCOM are largest when the model was forced with winds from NOGAPS-std. The bias becomes larger as one approaches the coast, i.e., where the land contamination increases (Figure 14). For example, biases from the model (HYCOM-MODAS) are $< 0.8^{\circ}\text{C}$ in the regions where the land contamination is $> 50\%$. The bias becomes much warmer, with a value of $\approx 1.6^{\circ}\text{C}$ ($\approx 2.0^{\circ}\text{C}$), in the regions where the land contamination of the winds is $> 80\%$ ($> 90\%$). In comparison, much smaller SST biases were obtained when HYCOM was forced with winds from NOGAPS-sea (NOGAPS-reg). The SST bias drops to about 0.3°C (-0.2°C) from about 2.0°C when the land contamination in winds is $> 90\%$.

The breakdown of the RMS errors between HYCOM and MODAS is also computed for all ocean, mask, and various land-sea mask class intervals (Figure 15). There is an obvious improvement in the model SSTs when using winds from NOGAPS-sea instead of those from NOGAPS-std. This is especially true in the regions where the land contamination in the NOGAPS-std winds is $> 70\%$, $> 80\%$ $> 90\%$. The most accurate SSTs are obtained when forcing HYCOM with winds from NOGAPS-reg everywhere, including the interior and the many different land-sea mask class intervals.

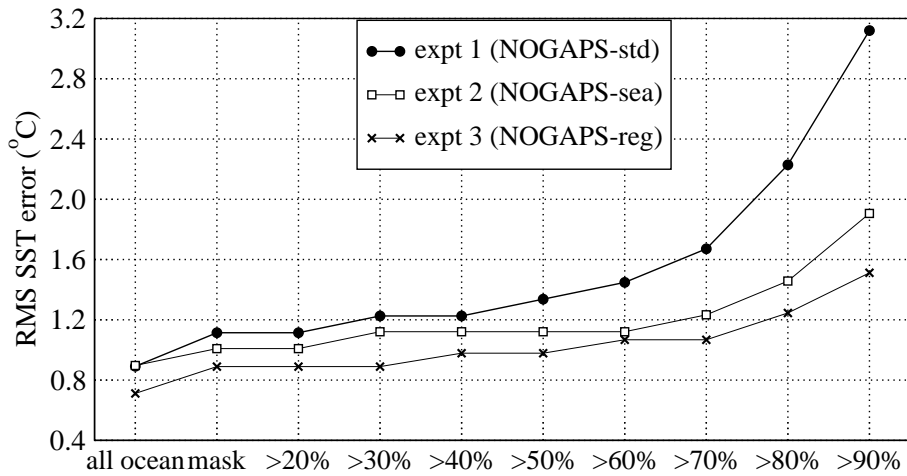


Fig. 15. The same as Figure 14 but for the RMS SST error.

5 Summary and Conclusions

There are two major motivations for writing this paper: (1) As of this writing, no study has quantified the impact of air-sea stratification on the satellite-based winds, typically calibrated to neutral winds at 10 m above the sea surface, over the Mediterranean Sea, and (2) shortcomings of winds from a coarse resolution NWP product ($1/2^\circ$) in forcing much finer resolution ($1/25^\circ$) OGCM have not been explored near the coastal boundaries of the Mediterranean Sea.

Concerning (1), we form mean winds from the twice-daily rain-free QSCAT wind measurements calibrated to the neutral atmospheric conditions over the Mediterranean Sea from 2000 through 2006. Stability-dependent winds are then computed at each 3 hourly time intervals based on an air-sea flux algorithm. Results demonstrate that the impact of air-sea stratification can be quite significant, giving monthly mean differences of $> 0.5 \text{ m s}^{-1}$ between neutral and stability-dependent winds in some regions. However, differences between the two generally do not exceed 0.2 m s^{-1} over the majority of the basin. The stability-dependent QSCAT winds are also compared to winds from an NWP product, NOGAPS, showing that both may differ near the land-sea boundaries. This is due mainly to the fact that NOGAPS winds over the sea are contaminated by those over the land. Such contamination is shown to be reduced by the creeping sea-fill methodology up to some extent, but we obtained more accurate NOGAPS winds based on QSCAT using the least squares approach, which is justified by the fact that both are strongly correlated to each other over the Mediterranean Sea.

As to (2), an eddy-resolving OGCM (HYCOM) was run using high temporal resolution (3 hourly) atmospheric forcing, including 10 m winds, from NOGAPS. Three model simulations use original, sea-filled and regression-corrected NOGAPS winds. All other forcing variables are identical in the simulations and there was no assimilation of any SST data nor relaxation to SST climatology. In comparison to a satellite-based SST product, SSTs from the model, which is forced with original NOGAPS winds, are generally inaccurate, giving a mean bias of $> 2^\circ\text{C}$ on monthly time scales. Such bias is largely removed from the model when using regression-corrected NOGAPS winds. While the correction based on QSCAT winds improve the accuracy of NOGAPS winds and thereby the performance of HYCOM in simulating SST, there are some regions that even QSCAT winds are not accurate. For example, the Aegean

Sea coastline is very irregular with many small islands. In such regions higher resolution NWP products may help, however, confirming their accuracy without satellite observations, such as QSCAT, will be challenging.

Acknowledgments

We would like to extend our special thanks to two anonymous reviewers for their helpful comments. HYCOM simulations were performed under the Department of Defense High Performance Computing Modernization Program on an IBM SP POWER3 at the Naval Oceanographic Office, Stennis Space Center, MS. This work is a contribution to the the 6.2 project, HYbrid Coordinate Ocean Model and Advanced Data Assimilation. This paper is contribution NRL/JA/7320/07/8047 and has been approved for public release.

Appendix I. Details of Mediterranean Sea Model Set Up.

I.1 Vertical Layers

The Mediterranean Sea HYCOM configured for this study used 20 hybrid layers. The target density values (in σ_t) corresponding to layers 1 through 20 are 19.50, 21.00, 22.50, 24.00, 25.50, 26.50, 27.25, 27.75, 28.15, 28.40, 28.60, 28.75, 28.90, 29.00, 29.05, 29.08, 29.11, 29.16, 29.18 and 29.22. This vertical layer structure was chosen to give isopycnal layers in the interior that increase in thickness or average with depth or layer number. The near-surface z -level regime is a natural consequence of HYCOM's minimum layer thickness. In this case, the minimum thickness of layer 1 is 3 m and this minimum thickness increases by $1.125\times$ per layer up to a maximum at 12 m, and the target densities are chosen such that at least the top four layers are in z -level coordinates.

The monthly mean temperature and salinity from the GDEM climatology are used to initialize the model. There is a relaxation to monthly mean SSS from GDEM. The reference mixed-layer thickness for the SSS relaxation is 30 m with the actual e-folding time depending on the actual mixed layer depth (MLD) ($30 \times 30/\text{MLD}$ days), i.e., it is more rapid when the MLD is shallow and less so when it is deep. This relaxation is to prevent long-timescale sea surface salinity drift.

The bottom topography was constructed from the 1 minute resolution data from the General Bathymetric Chart of the Oceans (GEBCO). Some hand-editing was performed to improve the coastline accuracy. The minimum depth at sea points was set to 5 m.

I.2 Atmospheric Forcing

The combination of accuracy and ease of computation makes the use of bulk formulae for sensible and latent heat fluxes preferred for computing air-sea fluxes in HYCOM (Kara et

al. 2005b). Including the air temperature and the model SST in the formulations for the latent and sensible heat flux automatically provides a physically realistic tendency towards the correct SST. The radiation flux (shortwave and net longwave fluxes) is highly dependent on cloudiness and is taken directly from NOGAPS.

HYCOM reads in a monthly mean climatological value of satellite-based attenuation coefficient for Photosynthetically Active Radiation (k_{PAR} in 1/m). The shortwave radiation at depth is then based on spatially-varying monthly k_{PAR} climatology (e.g., Kara et al., 2005a). The rate of heating/cooling of the model layers in the upper ocean is obtained from the net heat flux absorbed from the sea surface down to a depth, including water turbidity effects. The model treats rivers as an addition to the surface precipitation field. The river discharge is applied at individual coastal ocean grid points. The river discharge values are from the RivDIS monthly climatology (Vörösmarty et al., 1997), which gives river discharge values at the mouth of the river.

References

- Bourassa, M.A., Vincent, D.G., Wood, W.L., 1999. A flux parameterization including the effects of capillary waves and sea state. *J. Atmos. Sci.* 56, 1123–1139.
- Cavaleri, L., Bertotti, L., 1997. In search of the correct wind and wave fields in a minor basin. *Mon. Weather Rev.* 125, 1964–1975.
- Kara, A.B., Wallcraft, A.J., Hurlburt, H.E., 2005a. A new solar radiation penetration scheme for use in ocean mixed layer studies: An application to the Black Sea using a fine resolution HYbrid Coordinate Ocean Model (HYCOM). *J. Phys. Oceanogr.* 35, 13–32.
- Kara, A.B., Hurlburt, H.E., Wallcraft, A.J., 2005b. Stability-dependent exchange coefficients for air–sea fluxes. *J. Atmos. Oceanic Technol.* 22, 1077–1091.
- Kara, A.B., Wallcraft, A.J., Hurlburt, H.E., 2007. A correction for land contamination of atmospheric variables near land–sea boundaries. *J. Phys. Oceanogr.* 37, 803–818.
- Kara, A.B., Barron, C.N., 2007. Fine-resolution satellite-based daily sea surface temperatures over the global ocean. *J. Geophys. Res.* 112, C05041, doi:10.1029/2006JC004021.
- Kara, A.B., Wallcraft, A.J., Bourassa, M.A., 2008. Air–sea stability effects on the 10 m winds over the global ocean: Evaluations of air–sea flux algorithms. *J. Geophys. Res.* 113, C04009, doi:10.1029/2007JC004324.
- Large, W. G., Danabasoglu, G., Doney, S.C., McWilliams, J.C., 1997. Sensitivity to surface forcing and boundary layer mixing in a global ocean model: annual–mean climatology. *J. Phys. Oceanogr.* 27, 2418–2447.
- Liu, W.T., 2002. Progress in scatterometer application. *J. Oceanogr.* 58, 121–136
- Meissner, T., Smith, D., Wentz, F.J., 2001. A 10-year intercomparison between collocated SSM/I oceanic surface wind speed retrievals and global analyses. *J. Geophys. Res.* 106,

- Olita, A., Sorgente, R., Natale, S., Gabersek, S., Ribotti, A., Bonanno, A., Patti, B., 2007. Effects of the 2003 European heatwave on the Central Mediterranean Sea: surface fluxes and the dynamical response. *Ocean Science* 3, 273-289.
- Pinardi, N., Masetti, E., 2000. Variability of the large scale general circulation of the Mediterranean Sea from observations and modelling: a review. *Palaeogeography, Palaeoclimatology, Palaeoecology* 158, 153–173.
- Rosmond, T.E., João, T., Peng, M., Hogan, T.F., Pauley, R., 2002. Navy Operational Global Atmospheric Prediction System (NOGAPS): Forcing for ocean models. *Oceanography* 15, 99–108.
- Ruti, P.M, Marullo, S., D’Ortenzio, F.; Tremant, M., 2008. Comparison of analyzed and measured wind speeds in the perspective of oceanic simulations over the Mediterranean basin: Analyses, QuikSCAT and buoy data. *J. Mar. Sys.* 70, 33–48, doi: 10.1016/j.jmarsys.2007.02.026.
- Signell, R., Carniel, S., Cavaleri, L., Chiggiato, J., Doyle, J., Pullen, J., Scavo, M., 2005. Assessment of wind quality for oceanographic modeling in semi-enclosed basins. *J. Mar. Sys.* 53, 217–233.
- Uppala, S., coauthors, 2005. The ERA–40 re–analysis, *Quart. J. Roy. Meteor. Soc.* 131, 2961–3012. doi:10.1256/qj.04.176.
- Vörösmarty, C.J., Sharma, K., Fekete, B.M., Copeland, A.H., Holden, J., Marble, J., Lough, J.A., 1997. The storage and aging of continental runoff in large reservoir systems of the world. *Ambio* 26, 210–219.
- Weissman, D.E., Bourassa, M.A., Tongue, J., 2002. Effects of rain rate and wind magnitude on SeaWinds scatterometer wind speed errors. *J. Atmos. Oceanic Technol.* 19, 738-746.
- Wu, K., Haines, K., 1996. Modelling the dispersal of Levantine intermediate water and its role in Mediterranean deep water formation. *J. Geophys. Res.* 101, 6591–6607.
- Wu, C.L., Liu, Y., Kellogg, K.H., Pak, K.S., Glenister, R.L., 2003. Design and calibration of the SeaWinds scatterometer. *IEEE Trans. Aerospace Electronic Sys.* 39, 94–109.
- Zecchetto S., De Biasio, F., 2007. Sea surface winds over the Mediterranean basin from satellite data (2000-2004): meso- and local-scale features on annual and seasonal timescales. *J. App. Meteor. Clim.* 46, 814-827, doi: 10.1175/JAM2498.1.